ETH zürich

ETH Library

Contrasting spectral changes limit albedo impact on land-atmosphere coupling during the 2003 European heat wave

Journal Article

Author(s):
Teuling, A. J.; Seneviratne, Sonia I.

Publication date:
2008-02

Permanent link:
https://doi.org/https://doi.org/10.3929/ethz-c-000014365

Rights / license:
In Copyright - Non-Commercial Use Permitted

Originally published in:
Geophysical Research Letters 35(3), https://doi.org/10.1029/2007GL032778

This page was generated automatically upon download from the ETH Zurich Research Collection.
For more information, please consult the Terms of use.

Contrasting spectral changes limit albedo impact on land-atmosphere coupling during the 2003 European heat wave

A. J. Teuling[1] and S. I. Seneviratne[1]

Received 23 November 2007; revised 28 December 2007; accepted 3 January 2008; published 6 February 2008.

[1] Soil moisture related changes in the Earth's reflectance have been suggested to impact warm season climate variability through their direct impact on surface shortwave radiative forcing. Here we investigate the potential contribution of albedo to land-atmosphere coupling during the 2003 European heat wave. MODIS land surface albedo data for the years 2000–2004 are utilized to identify visible, near-infrared, and total shortwave anomalies for 2003. Changes in vegetation structure result in significant but contrasting albedo anomalies in the visible and near-infrared broadbands for most ecosystem types. Although locally the associated total shortwave radiative forcing can be significant (-10 W m^{-2}) especially over cropland areas, the effects almost cancel out at the sub-continental scale (-1 W m^{-2}). The net effect is too small to support the hypothesis that albedo impacts large-scale land-atmosphere coupling.
Citation: Teuling, A. J., and S. I. Seneviratne (2008), Contrasting spectral changes limit albedo impact on land-atmosphere coupling during the 2003 European heat wave, *Geophys. Res. Lett.*, *35*, L03401, doi:10.1029/2007GL032778.

1. Introduction

[2] Land surface albedo, defined as the ratio of reflected to downwelling (solar) radiation, is a key climate parameter for its direct control on the energy available at the land surface. Albedo is strongly variable, and depends (among many other factors) on wavelength, surface soil moisture, fractional vegetation cover and greenness. As radiative forcing associated with long-term albedo changes directly impact climate change, this issue has received considerable attention [e.g., *Myhre et al.*, 2005]. Albedo is also believed to contribute to land-atmosphere coupling on shorter timescales. In a landmark study, *Charney et al.* [1977] investigated the potential impact of albedo changes on the local climate caused by vegetation cover changes in the Sahel. *Eltahir* [1998] and *Brunsell* [2006] hypothesized that, through its positive feedback with surface net radiation, boundary layer moist static energy, and ultimately precipitation, albedo is a key component of the positive soil moisture-rainfall feedback. Albedo might be a negative actor in the soil moisture-temperature feedback, with high temperatures promoting enhanced drying, but concurrently decreasing net radiation and turbulent fluxes due to increased reflectance of the dry surface [*Wang and Davidson*, 2007; *Zaitchik et al.*, 2007].

[3] In a recent study, *Seneviratne et al.* [2006] have shown that soil moisture-atmosphere coupling, mostly through its impact on the Bowen ratio, can strongly impact temperature variability (and thus the occurrence of heat waves) in certain regions. In Europe, this effect was found to be strongest in the Mediterranean area in the late 20th century, and to be gradually strengthening in central and eastern Europe under the effects of global warming. Similarly, *Fischer et al.* [2007] showed that previous European heat waves, including the 2003 heat wave, were indeed significantly impacted by soil moisture anomalies. The contribution of albedo to soil moisture-atmosphere coupling remains however uncertain.

[4] Here we investigate the potential for drought-induced albedo changes (i.e., on intra-annual timescales) to contribute to land surface-atmosphere coupling on a (sub)continental scale through their impact on radiative forcing. We focus on the 2003 European heat wave for its unprecedented data availability and its large land surface water storage anomalies [*Andersen et al.*, 2005]. Even when only a limited number of observation years are available, the extremity of the event should accommodate detection of large-scale albedo anomalies.

2. Data

[5] Is this study we employ land surface albedo data from the Moderate Resolution Imaging Spectroradiometer (MODIS). We obtained the filled land surface albedo products [see *Moody et al.*, 2005] from the MODIS website (http://modis-atmos.gsfc.nasa.gov). These data are quality filtered and gaps are spatially interpolated by use of biome-dependent albedo statistics. Their spatial resolution is $1'$, and they are aggregated into 16-day periods for the years 2000–2004. The data are available for "white-sky" (bihemispherical reflectance under isotropic illumination) and "black-sky" (directional hemispherical reflectance at local solar noon) conditions. The actual albedo can be obtained by weighting the white and black sky albedos by the fraction of diffuse and direct radiation, respectively. Here we analyze black- and white-sky albedos in the following broadbands: visible (VIS, 0.3–0.7 μm), near-infrared (NIR, 0.7–5.0 μm), and total shortwave (SW, 0.3–5.0 μm). Since we found similar patterns for white and black sky albedo, only the results for white-sky albedo are presented.

[6] Also the filled Normalized Difference Vegetation Index (NDVI) product derived from MODIS is employed here. The reflectance spectrum of vegetation follows its morphological development, and the NDVI is a first-order diagnostic for this. It is computed from two (filled) spectral MODIS albedo products as:

$$\mathrm{NDVI} = \frac{\alpha_{0.86\mu\mathrm{m}} - \alpha_{0.67\mu\mathrm{m}}}{\alpha_{0.86\mu\mathrm{m}} + \alpha_{0.67\mu\mathrm{m}}} \quad (1)$$

[1]Institute for Atmospheric and Climate Science, ETH Zurich, Zurich, Switzerland.

Copyright 2008 by the American Geophysical Union.
0094-8276/08/2007GL032778

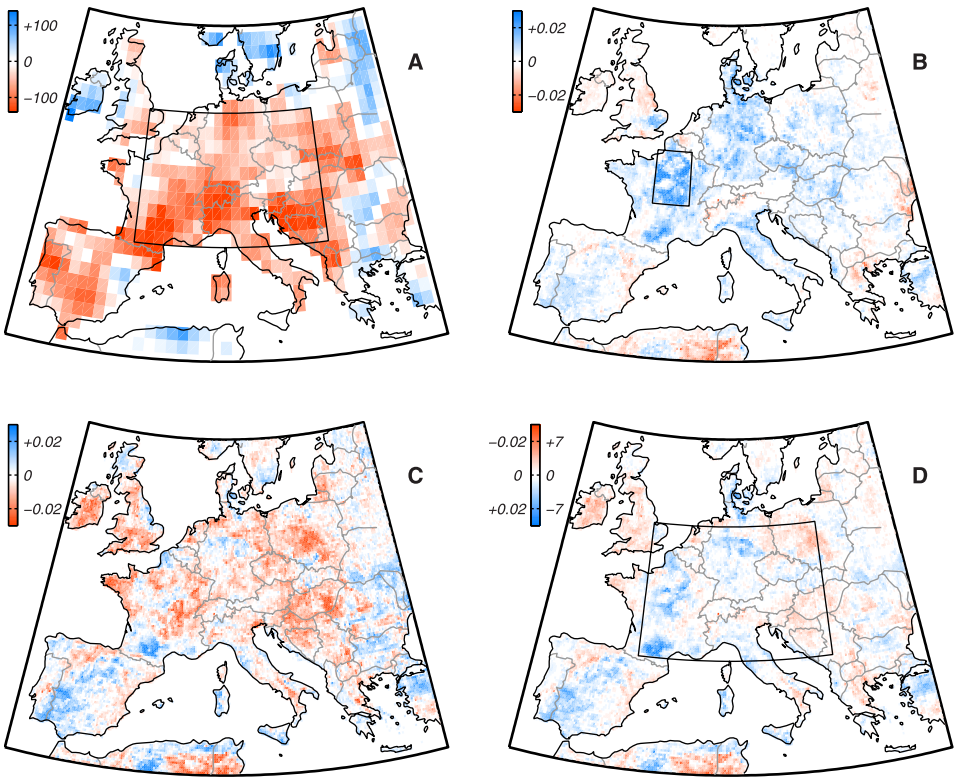

Figure 1. Climate and land surface albedo anomalies at the peak of the 2003 European heat wave (DOY 209–225). (a) Precipitation anomaly for April–July [mm]. (b) Broadband visible white sky albedo anomaly. (c) Broadband near-infrared white sky albedo anomaly. (d) Total shortwave albedo anomaly ($\Delta\alpha_{SW}$) and associated daily average clear-sky radiative forcing [W m^{-2}]. Note that +7 W m^{-2} corresponds to $\Delta\alpha_{SW} = -0.02$. Note that (b)–(d) have the same color scale. The data have been aggregated to a 10′ resolution for visualization only. Boxes indicate the selected sub-continental and regional scale areas used in the analysis.

where α is the spectral albedo and the subscript denotes the spectral wavelength. In addition, we use the 1′ land ecosystem classification product of the International Geosphere-Biosphere Programme (IGBP), which is derived from the official MODIS land ecosystem classification data set.

[7] Gridded monthly precipitation data (1°) were obtained from the Global Precipitation Climatology Centre (GPCC), operated by the German National Meteorological Service (http://www.dwd.de). For all products (MODIS and GPCC), we define an anomaly (Δ) as the difference between the value in 2003, and the "climatology" of the years 2000–2004 excluding 2003.

3. Results

[8] The 2003 heat wave was accompanied by a severe drought. Figure 1a shows the spatial distribution of rainfall anomalies in the months preceding the peak of the heat wave (April–July). In large parts of southern and central Europe the monthly rainfall deficits reached 50–100 mm. This is comparable to the storage anomalies reported by *Andersen et al.* [2005] using various methods. The low rainfall and high evaporative demand before and during the heat wave resulted in extreme low soil moisture across Europe. Since a decrease in surface soil moisture leads to increased reflectance of solar radiation by bare soil at all wavelengths [*Idso et al.*, 1975; *Lobell and Asner*, 2002] as well as reduced absorption of visible radiation by chlorophyll for plant photosynthesis, a positive albedo anomaly can be expected at least in the visible range.

[9] Figure 1b shows the distribution of $\Delta\alpha_{VIS}$ during one of the most severe stages of the 2003 heat wave (early August). Indeed, the drought conditions resulted in significant positive albedo anomalies in the visible range. The pattern is representative also for the later stages of the heat wave (see also Figure 2). The distribution of the positive anomalies roughly corresponds to that of the negative rainfall anomalies in the preceding months (Figure 1a), being largest in France, northern Italy, Germany, and parts of central Europe. However the magnitude of the albedo anomalies shows large regional differences. Their relation to land cover will be explored later. Large negative $\Delta\alpha_{VIS}$ are found locally in the Alps, which can likely be explained by increased snowmelt and/or increased vegetation productivity [*Jolly et al.*, 2005].

[10] The NIR albedo anomalies however show a very different picture. Over large parts of western Europe, negative NIR albedo anomalies dominate (Figure 1c). The $\Delta\alpha_{NIR}$ are of similar magnitude as the $\Delta\alpha_{VIS}$ in Figure 1b, but their sign is opposite. The distribution of NIR albedo anomalies is, however, somewhat different to that of $\Delta\alpha_{VIS}$. The processes leading to this opposite effect in the NIR may be of different types. One mechanism that leads to decreased NIR reflectance during senescence is the changes that occur in the mesophyll layer reducing the effectiveness

19448007, 2008, 3, Downloaded from https://agupubs.onlinelibrary.wiley.com/doi/10.1029/2007GL032778 by Eth Zurich, Wiley Online Library on [23/09/2025]. See the Terms and Conditions (https://onlinelibrary.wiley.com/terms-and-conditions) on Wiley Online Library for rules of use; OA articles are governed by the applicable Creative Commons License

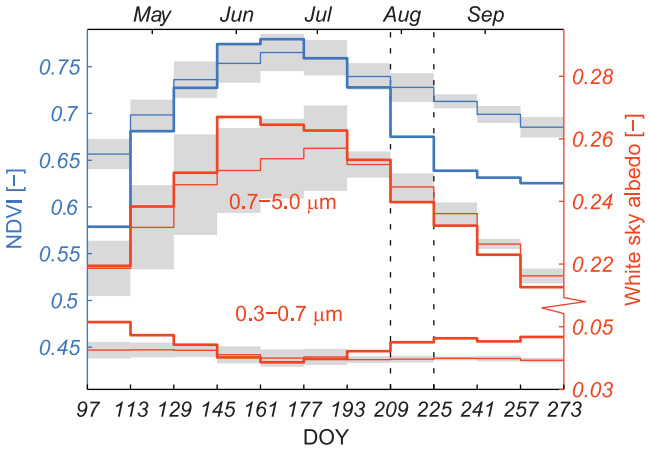

Figure 2. NDVI and white sky albedos for the year 2003 (thick lines) and climatology (thin lines) at the sub-continental scale (domain outlined in Figure 1a). Grey area indicates associated interannual variability. Note the discontinuity in the right *y*-axis. Dotted lines mark the 16-day period coinciding with the peak of the heat wave.

with which radiation at these wavelengths is reflected. Moreover, decrease of water in the plant tissues may lead to a decrease in turgescence and change in leaves' orientation, whereby a larger fraction of soil can be exposed; for plant cover with high reflectance in the NIR, this may lead to a net decrease in NIR (given lower NIR reflectance for soil). However, some processes may as well act against this observed change in NIR. For instance, soils increase their reflectance with decreasing soil moisture even stronger in the NIR range than in the VIS range [*Lobell and Asner*, 2002], and leaves generally show a similar response with decreasing leaf water content [*Carter*, 1991]. Thus, the MODIS retrievals suggest that the processes leading to a decrease of reflectance in the NIR dominated during the 2003 summer heat wave.

[11] In the resulting SW anomalies (Figure 1d), most of the variability in the VIS and NIR anomalies is averaged out. In parts of France and northern Germany local positive anomalies remain significant, while in parts of the Balkan and Poland the anomalies are predominantly negative although their absolute magnitude is somewhat smaller. Next, we focus on the temporal dynamics of albedo during the 2003 heat wave.

[12] The growing season evolution of α_{VIS} and α_{NIR} at the sub-continental scale is plotted in Figure 2. Clearly, the dynamic range (and associated interannual variability) is much larger for α_{NIR} than for α_{VIS}. In late spring and early summer, positive anomalies in α_{NIR} may reflect an enhanced vegetation greenup in response to early spring warmth [*Zaitchik et al.*, 2006]. From mid-July onward, α_{NIR} and α_{VIS} display the above-mentioned characteristics (negative $\Delta\alpha_{NIR}$, positive $\Delta\alpha_{VIS}$), indicating water stress in the vegetation. Whereas $\Delta\alpha_{VIS}$ by far exceeds the interannual variability, this is not true for $\Delta\alpha_{NIR}$.

[13] For comparison, also the evolution of the NDVI (Equation 1) is plotted. Its relationship to α_{VIS} and α_{NIR} can help to understand the underlying processes. Interestingly, the NDVI anomalies are negative in spring and positive in June. From August on, large negative anomalies dominate (due to the contrasting anomalies in the α_{VIS} and α_{NIR}). While the negative NDVI anomalies in spring are mainly located in the north-western part of our sub-continental domain, the summer anomalies occur mainly in the south-eastern part (not shown). The correspondence in both seasonal cycle and anomalies of NIR albedo and NDVI (in particular the stronger negative anomalies in mid-summer to fall) is a further indication that the NIR albedo anomalies are linked to vegetation stress rather than enhanced soil drying.

[14] Due to the heterogeneity of the European land cover, it is of interest to investigate how the albedo anomalies are distributed among different ecosystem types. This is done for the larger (sub-continental) scale, and a smaller (regional-scale) domain where the albedo changes are the largest (Figure 1b). Figure 3b shows the distribution of cropland in Europe as derived from the IGBP data set. Although this data set is also used for the processing of the MODIS albedos, we believe the correspondence discussed hereafter is not an artifact of the data set since we focus on anomalies patterns rather than patterns in the albedo itself. Clearly, there is a large correspondence between cropland density and $\Delta\alpha_{VIS}$, $\Delta\alpha_{NIR}$, and $\Delta\alpha_{SW}$ (Figures 1b–1d). Table 1 confirms that, at both scales (Panels A and B), the largest spectral albedo changes are primarily associated with croplands and evergreen broadleaf forest. Note that these two classes also have relatively low NDVI. Since croplands are also the dominating ecosystem type in both focus areas (38.5% and 56.6%, respectively, see also Figure 3), they are the albedo anomaly "hot-spots". The anomalies are nearly twice as large at the regional scale as on the sub-continental scale. Within most classes, a positive $\Delta\alpha_{VIS}$ is almost completely balanced by a negative $\Delta\alpha_{NIR}$. Only at the smaller regional scale (Table 1, Panel B) the croplands NIR anomalies are much smaller in magnitude than the VIS anomalies. Note also that the α_{SW} product has its own errors and weighting, so its anomalies not necessarily equal the sum of $\Delta\alpha_{VIS}$ and $\Delta\alpha_{NIR}$.

[15] Any effects of land surface albedo on land-atmosphere interaction occur through the shortwave radiation budget. Therefore, we evaluate the impact of interannual albedo dynamics on the land surface energy

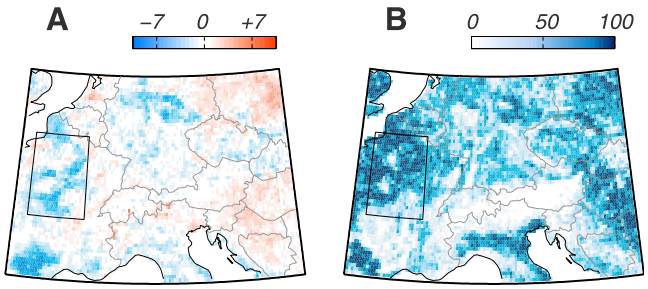

Figure 3. Albedo anomaly "hot-spots" at the sub-continental scale. (a) Inset from Figure 1d. (b) Distribution of croplands, expressed as the percentage of pixels in IGBP classes 12 and 14 (see Table 1).

19448007, 2008, 3, Downloaded from https://agupubs.onlinelibrary.wiley.com/doi/10.1029/2007GL032778 by Eth Zurich, Wiley Online Library on [23/09/2025]. See the Terms and Conditions (https://onlinelibrary.wiley.com/terms-and-conditions) on Wiley Online Library for rules of use; OA articles are governed by the applicable Creative Commons License

Table 1. Relation Between IGBP Ecosystem Classification and 2003 VIS, NIR, and SW Albedo Anomalies $\Delta\alpha$ (DOY 209–225). Also the NDVI for the Period is Given[a]

IGBP Class	Description	Cover,[b] %	NDVI	$\Delta\alpha_{VIS}$	$\Delta\alpha_{NIR}$	$\Delta\alpha_{SW}$
	Panel A: Sub-continental Scale					
2	evergreen broadleaf forest	2.0	0.70	0.010	−0.010	0.002
4	deciduous broadleaf forest	6.7	0.81	0.003	−0.004	0.000
5	mixed forests	19.5	0.80	0.002	−0.003	0.000
8	woody savannas	6.4	0.71	0.005	−0.005	0.001
12	croplands	38.5	0.59	0.010	−0.008	0.002
13	urban and built-up	5.1	0.57	0.005	−0.003	0.002
14	cropland/natural vegetation mosaic	9.4	0.70	0.006	−0.007	0.001
	average			0.007	−0.006	0.002
	Panel B: Regional Scale					
2	evergreen broadleaf forest	6.2	0.61	0.018	−0.016	0.004
4	deciduous broadleaf forest	3.9	0.82	0.004	−0.000	0.003
5	mixed forests	7.7	0.83	0.003	−0.000	0.002
8	woody savannas	3.9	0.68	0.011	−0.007	0.004
12	croplands	56.6	0.52	0.019	−0.006	0.008
13	urban and built-up	3.3	0.53	0.007	−0.002	0.003
14	cropland/natural vegetation mosaic	12.0	0.68	0.011	−0.007	0.004
	average			0.016	−0.006	0.007

[a]Only ecosystems with a cover fraction over 5% are listed. All statistics are calculated based on equal-area reprojection of the original data.
[b]Percentage of land pixels.

budget by the difference in net surface shortwave radiative forcing ΔR^*_{SW}:

$$\Delta R^*_{SW} = -\Delta\alpha_{SW} R_{SW}\downarrow, \quad (2)$$

where $\Delta\alpha_{SW}$ is the total shortwave (0.3–5.0 μm) albedo anomaly, and $R_{SW}\downarrow$ the (daily average) downwelling shortwave radiation. Daily $R_{SW}\downarrow$ is highly dependent on cloud cover, and also shows a slight decrease with latitude. For simplicity, we adopt a uniform value for $R_{SW}\downarrow$ of 350 W m^{-2} corresponding to clear sky conditions typical for the 2003 heat wave [see *Zaitchik et al.*, 2006, Table V]. The distribution of ΔR^*_{SW} is shown in Figure 1d. The radiative forcing is relatively small in most of the area affected by the heat wave, although locally ΔR^*_{SW} reaches −10 W m^{-2}. At larger scales however, these differences are compensated by opposite anomalies in other areas. Using the average $\Delta\alpha_{SW}$ values in Table 1, we find values for ΔR^*_{SW} of −0.7 and −2.5 W m^{-2} at the sub-continental and regional scale, respectively.

4. Discussion and Conclusions

[16] Land surface albedo in the visible and near-infrared broadbands is found to respond in opposite ways to the anomalous soil moisture conditions associated with the 2003 European heat wave. While enhanced soil drying alone would increase land surface reflectance, this effect is largely masked by changes in vegetation characteristics in response to water stress, resulting in contrasting changes in spectral reflectance. Our results agree with the findings of *Zaitchik et al.* [2006] regarding albedo anomalies during the 2003 heat wave, but offer a more detailed view in terms of the spatial, temporal, and spectral variability. They are also consistent with the small contribution of albedo to soil moisture-driven changes in the surface energy budget reported by *Small and Kurc* [2003] for semiarid conditions.

[17] The most significant total shortwave albedo anomalies are found for croplands, which is also the dominant ecosystem type in western Europe. This is consistent with recent results of *Zaitchik et al.* [2007] for the Middle East. Locally, the radiative forcing associated with the shortwave albedo anomalies might modulate mesoscale feedbacks, but at the sub-continental scale this effect becomes too small to significantly impact land surface-atmosphere coupling. Thus our results do not support the hypothesis of possibly significant drought-induced albedo feedbacks, at least in the case of the European 2003 heat wave. If models are to capture the dynamics of albedo in response to soil moisture variations, they should account not only for soil moisture effects on albedo, but also for the complex spectral response of vegetation to water stress.

[18] **Acknowledgments.** A.J.T. acknowledges financial support from the Netherlands Organisation for Scientific Research (NWO) through a Rubicon grant. The authors thank Reto Stöckli, Andreas Roesch, Gabriela Schaepman, and Bernard Pinty for their useful comments.

References

Andersen, O. B., S. I. Seneviratne, J. Hinderer, and P. Viterbo (2005), GRACE-derived terrestrial water storage depletion associated with the 2003 European heat wave, *Geophys. Res. Lett.*, *32*(18), L18405, doi:10.1029/2005GL023574.

Brunsell, N. A. (2006), Characterization of land-surface precipitation feedback regimes with remote sensing, *Remote Sens. Environ.*, *100*, 200–211, doi:10.1016/j.rse.2005.10.025.

Carter, G. A. (1991), Primary and secondary effects of water content on the spectral reflectance of leaves, *Am. J. Bot.*, *78*, 916–924.

Charney, J., W. J. Quirk, S. Chow, and J. Kornfield (1977), A comparative study of the effects of albedo change on drought in semi-arid regions, *J. Atmos. Sci.*, *34*, 1366–1385.

Eltahir, E. A. B. (1998), A soil moisture-rainfall feedback mechanism: 1. Theory and observations, *Water Resour. Res.*, *34*, 765–776.

Fischer, E. M., S. I. Seneviratne, D. Lüthi, and C. Schär (2007), Contribution of land-atmosphere coupling to recent European summer heat waves, *Geophys. Res. Lett.*, *34*, L06707, doi:10.1029/2006GL029068.

Idso, S. B., R. D. Jackson, R. J. Reginato, B. A. Kimball, and F. S. Nakayama (1975), The dependence of bare soil albedo on soil water content, *J. Appl. Meteorol.*, *14*, 109–113.

Jolly, W. M., M. Dobbertin, N. E. Zimmermann, and M. Reichstein (2005), Divergent vegetation growth responses to the 2003 heat wave in the Swiss Alps, *Geophys. Res. Lett.*, *32*, L18409, doi:10.1029/2005GL023252.

Lobell, D. B., and G. P. Asner (2002), Moisture effects on soil reflectance, *Soil Sci. Soc. Am. J.*, *66*, 722–727.

19448007, 2008, 3, Downloaded from https://agupubs.onlinelibrary.wiley.com/doi/10.1029/2007GL032778 by Eth Zurich, Wiley Online Library on [23/09/2025]. See the Terms and Conditions (https://onlinelibrary.wiley.com/terms-and-conditions) on Wiley Online Library for rules of use; OA articles are governed by the applicable Creative Commons License

Moody, E. G., M. D. King, S. Platnick, C. B. Schaaf, and F. Gao (2005), Spatially complete global spectral surface albedos: Value-added datasets derived from Terra MODIS land products, *IEEE Trans. Geosci. Remote Sens.*, *43*, 144–158.

Myhre, G., M. M. Kvalevåg, and C. B. Schaaf (2005), Radiative forcing due to anthropogenic vegetation change based on MODIS surface albedo data, *Geophys. Res. Lett.*, *32*, L21410, doi:10.1029/2005GL024004.

Seneviratne, S. I., D. Lüthi, M. Litschi, and C. Schär (2006), Land-atmosphere coupling and climate change in Europe, *Nature*, *443*, 205–209, doi:10.1038/nature05095.

Small, E. E., and S. A. Kurc (2003), Tight coupling between soil moisture and the surface radiation budget in semiarid environments: Implications for land-atmosphere interactions, *Water Resour. Res.*, *39*(10), 1278, doi:10.1029/2002WR001297.

Wang, S., and A. Davidson (2007), Impact of climate variations on surface albedo of a temperate grassland, *Agric. For. Meteorol.*, *142*, 133–142, doi:10.1016/j.agrformet.2006.03.027.

Zaitchik, B. F., A. K. Macalady, L. R. Bonneau, and R. B. Smith (2006), Europe's 2003 heat wave: A satellite view of impacts and land-atmosphere feedbacks, *Int. J. Climatol.*, *26*, 743–769, doi:10.1002/joc.1280.

Zaitchik, B. F., J. P. Evans, R. A. Geerken, and R. B. Smith (2007), Climate and vegetation in the Middle East: Interannual variability and drought feedbacks, *J. Clim.*, *20*, 3924–3941, doi:10.1175/JCLI4223.1.

S. I. Seneviratne and A. J. Teuling, Institute for Atmospheric and Climate Science, CHN N 16.2, Universitätstrasse 16, CH-8092 Zürich, Switzerland. (ryan.teuling@env.ethz.ch)

19448007, 2008, 3, Downloaded from https://agupubs.onlinelibrary.wiley.com/doi/10.1029/2007GL032778 by Eth Zurich, Wiley Online Library on [23/09/2025]. See the Terms and Conditions (https://onlinelibrary.wiley.com/terms-and-conditions) on Wiley Online Library for rules of use; OA articles are governed by the applicable Creative Commons License